

Interferometric characterization of density dynamics of an ultradense Z-pinch plasma^{a)}

John G. Ackenhusen^{b)} and David R. Bach

Laser Plasma Interaction Laboratory, The University of Michigan, Ann Arbor, Michigan 48109

(Received 23 March 1978; accepted for publication 3 October 1978)

We have measured the spatially and temporally resolved density in a Z-pinch plasma by holographic interferometry. The high electron density ($4 \times 10^{19} \text{ e/cm}^3$), short density scale length ($100 \mu\text{m}$), and low temperature (about 20 eV) make the plasma source suitable for simulation of laser-pellet interaction experiments at $10.6\text{-}\mu\text{m}$ laser wavelengths. A cinema of density evolution, indicating plasma pinching and subsequent relaxation, provides an experimental view of plasma dynamics which is then compared to simple theoretical models.

PACS numbers: 52.55.Ez, 52.70.Kz, 42.40.My

This letter presents interferometric measurements of the spatially and temporally resolved electron density of a Z-pinch plasma and provides an experimental characterization of the dynamics of the Z-pinch device. Theoretical modeling of plasma evolution in the linear Z pinch has been treated in the literature¹ and experiments determining peak or average electron densities and temperatures have been performed.^{2,3} However, no detailed study of the evolution process of the Z-pinch plasma has yet been reported. The evolution of the Z-pinch plasma is useful to examine for comparison to theoretically postulated pinch dynamics and for investigation of its use as a plasma source for laser fusion simulation experiments.

Certain Z-pinch design considerations⁴ allow achievement of peak densities of $4 \times 10^{19} \text{ e/cm}^3$ (four times critical density for $10.6\text{-}\mu\text{m}$ -wavelength CO_2 laser light), low electron temperature (around 20 eV), and short critical scale lengths ($L = n_c / \nabla n_e = 100\text{--}200 \mu\text{m}$). Such a plasma is particularly well suited for experimental studies of nonlinear laser-plasma interactions, as the short density scale length and low temperature allow achievement of the field-strength condition $V_{\text{osc}}/V_{\text{th}} = 1$ (V_{osc} is the electron quiver velocity in oscillating laser electric field at critical layer and V_{th} is the electron thermal velocity) at a relatively modest CO_2 laser intensity of $2 \times 10^{11} \text{ W/cm}^2$. Thus, at the critical layer of such a plasma, the laser radiation pressure may exceed the plasma kinetic pressure and modify the plasma density in the manner of current research interest in laser-induced fusion. In addition, because the plasma column diameter is much greater than the laser focal spot size, slab geometry may often be used to simplify theoretical considerations. This laser-pellet-like plasma has the additional advantage of being produced separately from the laser to allow accurate characterization of the initial state of the target plasma in the absence of the laser.

The design details of the Z-pinch plasma source have been reported earlier.⁴ The Z-pinch chamber was 17 cm long, 1.5 cm in radius, and filled to 1.4 Torr with helium. This vertical column was mounted upon a $14\text{-}\mu\text{F}$ energy storage capacitor which was charged to 12.75 kV. The current discharge was initiated by a triggered spark gap and had a ringing period of $8 \mu\text{sec}$. Plasma pinching occurred 900 nsec after discharge initiation, and current through the plasma at the time of the pinch was 80 kA. Diagnostics indicated a fully doubly ionized plasma with an electron temperature of about 20 eV at the pinch time.

Four beam ports around the waist of the column allowed entrance and exit of the radially incident high-intensity CO_2 laser beam and the object beam of a holographic interferometer (Fig. 1).

The pulsed holographic interferometer, designed and described by Rockett,⁵ used a frequency-doubled ruby laser pulse ($\lambda = 347.2 \text{ nm}$) of 16 nsec full width at half maximum (FWHM). Interferograms were taken perpendicular to the

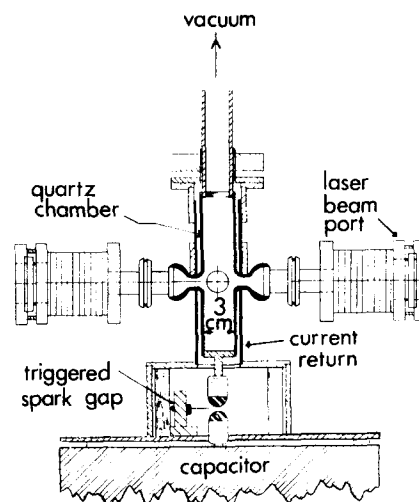


FIG. 1. Z-pinch target chamber. Current flow, initiated from capacitor by spark gap, proceeds upward through helium-filled quartz cylinder and returns downward to ground through the coaxial outer copper cylinder.

^{a)}Supported in part by The National Science Foundation, the Air Force Office of Scientific Research, and The University of Michigan College of Engineering.

^{b)}Permanent address: Bell Laboratories, Murray Hill, N.J. 07974.

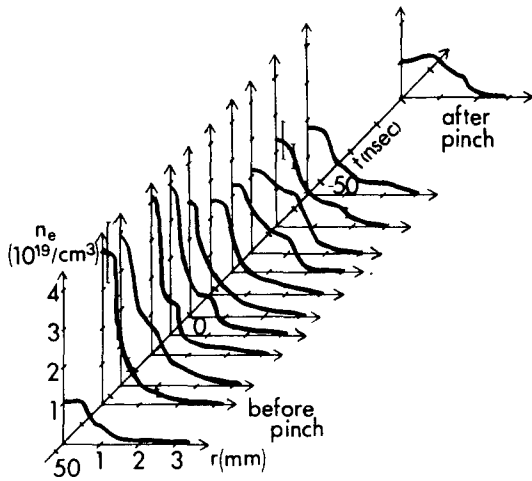


FIG. 2. Electron density versus radius r and time t displaying evolution of discharge plasma. Data points were spaced less than 0.1 mm. apart.

axis of the plasma column, and radial and axial density profiles were extracted by Abel inversion of fringe shift information.

The time of peak plasma compression was marked by a 150-nsec FWHM burst of optical continuum radiation. This served as a timing mark from which the time of the interferometer laser pulse was measured. This time interval t between the pinch and the interferometer pulse was varied on successive shots to obtain a series of "snapshots" describing density evolution.

Figure 2 presents radial electron-density profiles at a constant axial position on the plasma column as a function of time. The zero point in time corresponds to time of peak optical emission, and positive values of t relate to times prior to optical peak.

The plasma reached critical density for 10.6- μm radiation (10^{19} e/cm^3) at about 50 nsec before time of pinch and remained overdense until 80 nsec following the pinch time. As the plasma proceeded toward pinch, centerline density

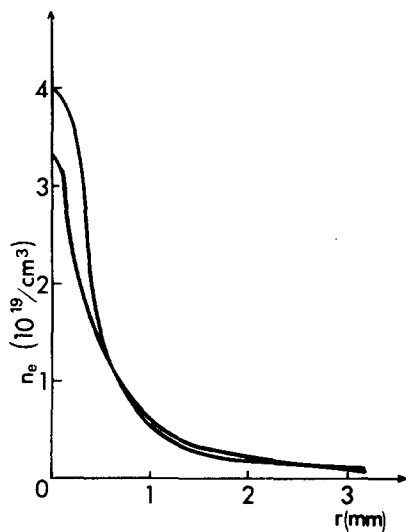


FIG. 3. Electron density versus radius at pinch time ($t = 0$) for two different shots, showing reproducibility of discharge.

built up quickly, and for $25 > t > 0$ nsec, the buildup of a density step in the region of $n_e = 1 \times 10^{19} \text{ e/cm}^3$ provided a short critical scale length ($L \simeq 70 \mu\text{m}$). At times immediately preceding $t = 0$, a quasistationary density profile was reached, characterized by a peak centerline density of $4 \times 10^{19} \text{ e/cm}^3$ and a density shelf at a radius of 0.6 mm. Immediately after the pinch time ($0 > t > -30$ nsec), a second quasistationary profile was reached in which the density shelf had smoothed out to provide a longer critical scale length ($100 \mu\text{m} < L < 200 \mu\text{m}$). This was followed by a full relaxation from the pinch.

Reproducibility of the Z pinch was essential to this measurement of plasma evolution by successive Z-pinch firings. To determine shot-to-shot reproducibility, three to six shots were taken with the interferometer pulse at a fixed stage of plasma evolution for each profile presented in Fig. 2. Figure 3 compares density profiles taken at the same stage of plasma evolution on two different shots. For radii greater than 0.5 mm, densities were reproducible to within 10%. Toward the center of the plasma ($r < 0.5$ mm), shot-to-shot density variation appeared greater. However, due to the nature of the fringe reading and Abel inversion processes, density uncertainty near the column centerline was larger (about 30%) than that in the region where $n = 10^{19} \text{ e/cm}^3$ (about 10%).

By obtaining density profiles at several axial positions on a single interferogram, a characterization of the z dependence of density was obtained. A plot of $n(r, z)$ at the pinch time ($t = 0$) is displayed in Fig. 4. Since this interferogram was taken at the pinch time when radial motion had ceased, it proved interesting to compare the profile with that of the Bennett distribution for the equilibrium pinch.⁶ The Bennett relation, derived from the balance of plasma kinetic pressure at a given electron temperature θ_e with the magnetic pres-

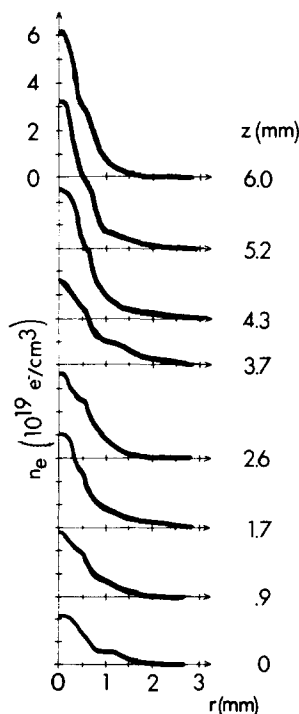


FIG. 4. Electron density versus radius r and axial position z at pinch time ($t = 0$). Note general increase in centerline density for higher values of z .

sure from the current-induced magnetic field, predicts a density profile of the form:

$$n(r) = n_0 / (1 + n_0 b r^2)^2, \quad (1)$$

$$b = \mu_0 e^2 v_d^2 / 8(\theta_e + \theta_i / Z), \quad (2)$$

where n_0 is the peak density and v_d is the electron drift velocity due to the current flow. The plots of $n(r, z)$ at various axial positions were normalized to obtain a constant centerline density n_0 of $2.1 \times 10^{19} \text{ e/cm}^3$. The scaled profiles were then plotted on a common coordinate system (Fig. 5). The solid curve is a Bennett profile, as given above, for $n_0 = 2.1 \times 10^{19} \text{ e/cm}^3$, $\theta_e = \theta_i = 12.2 \text{ eV}$, $Z = 2$, and $v_d = 2 \times 10^5 \text{ cm/sec}$. The drift velocity was calculated from the pinch discharge current uniformly distributed across the column at density per unit length (e/cm^2) indicated by the interferograms. However, more sophisticated numerical calculations⁷ have indicated the presence of a shell-like current distribution.

Examination of holographic interferograms indicated the wavelike propagation of a high-density region in the direction of the electron current carriers. The propagation velocity was 10^6 cm/sec , and both plasma pinching and relaxation from pinch occurred as an axially propagating wave rather than as a simultaneous axially independent process.

Evidently, simple one-dimensional treatments of Z-pinch dynamics were not sufficient to predict the experimentally observed manner of pinching and relaxation. A one-dimensional magnetohydrodynamic numerical simulation predicted the full ionization, the density profile at the pinch time in the region of critical radius, and the time to pinch to within experimental accuracy.⁸ However, the density "shelf" near the 1-mm radius, the presence of z gradients, and the propagation of an axial density wave indicated that two-dimensional effects were important in evolution.

We have described the evolution of a plasma produced by a small linear Z-pinch discharge with the intent of exploring its use as a laser-pellet-simulation target. The time scale of the Z-pinch evolution was found to be large compared to typical laser-pulse lengths, so evolution effects could be neglected during laser-pulse time. The target density profile was very dependent upon time of laser incidence relative to the pinch time, allowing for the selection of a variety of den-

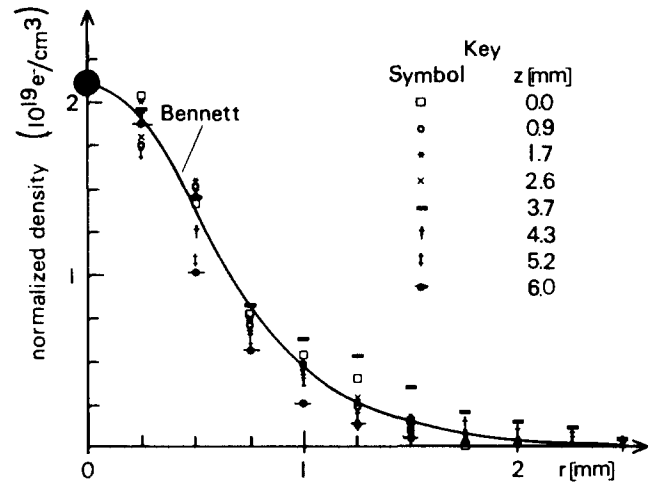


FIG. 5. Electron-density profiles of Fig. 4 normalized to common centerline density of $2.1 \times 10^{19} \text{ e/cm}^3$, superposed on Bennett profile for equilibrium pinch at ion and electron temperature of 12.2 eV.

sity profiles. Furthermore, the column diameter was large compared to typical diffraction-limited focal spot sizes; therefore, theoretical comparisons could often be simplified to one-dimensional slab geometry. This plasma source has been used to study a variety of nonlinear laser-plasma interaction effects.⁹

It is a pleasure to acknowledge experimental and theoretical assistance from Dr. J. Duderstadt, Dr. D. Duston, D. Kania, Dr. P. Rockett, Dr. D. Steel, and D. Voss.

¹Y. Hashino, H. Suemitsu, and K. Fukuda, *Jpn. J. Appl. Phys.* **11**, 710 (1972); J.W. Shearer, University of California Internal Report UCID-16973, 1975 (unpublished).

²H. Zwicker and U. Schumacher, *Z. Phys.* **183**, 435 (1955).

³D.E. Roberts, *Phys. Fluids* **15**, 192 (1972).

⁴D.G. Steel, P.D. Rockett, D.R. Bach, and P.L. Colestock, *Rev. Sci. Instrum.* **49**, 456 (1978).

⁵P.D. Rockett, Ph.D. dissertation (University of Michigan, 1977) (unpublished).

⁶M.A. Uman, *Introduction to Plasma Physics* (McGraw-Hill New York, 1964), p. 189.

⁷D. Duston and J.J. Duderstadt, *Phys. Rev. A* (to be published).

⁸D. Duston, P.D. Rockett, D.G. Steel, J.G. Ackenhusen, D.R. Bach, and J.J. Duderstadt, *Appl. Phys. Lett.* **31**, 801 (1977).

⁹P.D. Rockett, D.G. Steel, J.G. Ackenhusen, and D.R. Bach, *Phys. Rev. Lett.* **40**, 649 (1978); J.G. Ackenhusen and D.R. Bach, *Appl. Phys. Lett.* (to be published).